The EMBO Journal Vol.18 No.7 pp.1793–1804, 1999

Assembly of thick filaments and myofibrils occurs in the absence of the myosin head

Richard M.Cripps[1], Jennifer A.Suggs and Sanford I.Bernstein[2]

Department of Biology and Molecular Biology Institute, San Diego State University, San Diego, CA 92182-4614, USA

[1]Present address: Department of Biology, University of New Mexico, Albuquerque, NM 87131-1091, USA

[2]Corresponding author
e-mail: sbernst@sunstroke.sdsu.edu

We investigated the importance of the myosin head in thick filament formation and myofibrillogenesis by generating transgenic *Drosophila* lines expressing either an embryonic or an adult isoform of the myosin rod in their indirect flight muscles. The headless myosin molecules retain the regulatory light-chain binding site, the α-helical rod and the C-terminal tailpiece. Both isoforms of headless myosin co-assemble with endogenous full-length myosin in wild-type muscle cells. However, rod polypeptides interfere with muscle function and cause a flightless phenotype. Electron microscopy demonstrates that this results from an antimorphic effect upon myofibril assembly. Thick filaments assemble when the myosin rod is expressed in mutant indirect flight muscles where no full-length myosin heavy chain is produced. These filaments show the characteristic hollow cross-section observed in wild type. The headless thick filaments can assemble with thin filaments into hexagonally packed arrays resembling normal myofibrils. However, thick filament length as well as sarcomere length and myofibril shape are abnormal. Therefore, thick filament assembly and many aspects of myofibrillogenesis are independent of the myosin head and these processes are regulated by the myosin rod and tailpiece. However, interaction of the myosin head with other myofibrillar components is necessary for defining filament length and myofibril dimensions.

Keywords: *Drosophila*/muscle/myofibril/myosin/thick filament

Introduction

During muscle development, the synthesis and assembly of myofibrillar components are precisely regulated to yield filaments and sarcomeres of defined geometry. Myosin molecules assemble into hexamers, composed of two myosin heavy chains (MHCs) and four light chains, that polymerize into thick filaments of specific dimensions. Thick filaments in turn are organized into the A-band of the muscle sarcomere, where they interdigitate with thin filaments to yield myofibrils with uniform sarcomere length and diameter. The globular heads of the myosin molecules projecting from the thick filaments power muscle contraction via ATP-dependent interaction with the actin-containing thin filaments. Although some insights into myofilament assembly and interaction have resulted from *in vitro* studies, the protein domains involved in orchestrating *in vivo* myofibril assembly are largely unknown.

The ability of native myosin to form thick filaments *in vitro* (Huxley, 1963; Moos *et al.*, 1975) permits analysis of myosin subfragments that are capable of, or required for, filament assembly. Myosin rods can assemble into filaments and other higher-ordered structures *in vitro* (Lowey *et al.*, 1969) indicating that the primary determinant of filament formation lies in this part of the molecule. Recent studies identified a small region near the C-terminus of the rod that is required for normal assembly (Nyitray *et al.*, 1983; Maeda *et al.*, 1989; Sohn *et al.*, 1997), and a conserved 29 amino acid domain of a skeletal muscle myosin rod is both required and sufficient for assembly of myosin subfragments into higher-ordered structures (Sohn *et al.*, 1997). A difficulty with the interpretation of many of these experiments is that although myosin fragments can assemble into insoluble structures, many do not form true filaments and instead accumulate into paracrystals. Furthermore, the *in vitro* formation of these structures is markedly dependent upon temperature, pH and ionic conditions, making it difficult to apply the conclusions obtained to the *in vivo* situation (reviewed in Davis, 1988; Bandman *et al.*, 1997).

Hoppe and Waterston (1996) used an *in vivo* approach to mapping MHC rod domains critical to thick filament assembly in body wall muscles of *Caenorhabditis elegans*. They demonstrated that either of two regions in the rod of one isoform of MHC is necessary for thick filament formation. These regions may contain amino acid residues that permit antiparallel interactions required for thick filament nucleation.

The role of the myosin head in thick filament and myofibril assembly *in vivo* is uncertain. A naturally occurring isoform of *Drosophila* MHC contains a novel N-terminal extension fused to the rod and tailpiece of full-length MHC (Standiford *et al.*, 1997). This molecule co-assembles with full-length MHC into muscle fibers, indicating that all myosin molecules within a thick filament need not have a globular head for filament and myofibril assembly to proceed *in vivo*. In contrast, data from *C.elegans* attest to an important function for the myosin head in thick filament assembly. Mutations in the *C.elegans unc-54* MHC gene strongly interfere with assembly of both wild-type and mutant MHC into thick filaments (Bejsovec and Anderson, 1988). Many of the lesions are in functionally important domains of the myosin head, including the binding sites for ATP and actin (Bejsovec and Anderson, 1990). These studies suggest that myosin

with a functionless head does not assemble into thick filaments and such molecules may interfere with the association of normal MHC into thick filaments. Thus, although the myosin rod is capable of assembly *in vitro* into thick filament-like structures, the function of the myosin head may be required *in vivo* for normal filament formation.

Thick filaments co-assemble with thin filaments and other myofibrillar proteins to form sarcomeres during muscle development. A number of myosin-binding proteins affect the organization of thick filaments formed either *in vitro* or in non-muscle cells (Moos *et al.*, 1975; Seiler *et al.*, 1996) and several myosin-binding proteins are thought to be important to sarcomere assembly in muscle (reviewed in Epstein and Fischman, 1991). Regions of myosin that bind these proteins can be determined through *in vitro* solid-phase binding assays (see for example Labeit *et al.*, 1992; Obermann *et al.*, 1997), but whether these domains are critical to sarcomere assembly is not known. Since myofibrillogenesis has not been reproduced outside of a muscle cell, it is not possible to approach this question using an *in vitro* system.

Here we describe a model system designed to address questions of thick filament and myofibril assembly in muscle cells in an intact organism. We produced transgenic *Drosophila* lines whose indirect flight muscles (IFMs) express one of two different isoforms of MHC that are N-terminally truncated and therefore lack the enzymatic function of the myosin head. These molecules retain the regulatory light-chain binding site, the myosin rod and the C-terminal tailpiece. We studied the functional properties of these molecules both in a wild-type background and in a mutant background where no endogenous MHC is produced in the IFMs.

Using this system we show that both embryonic and adult headless myosin molecules can co-assemble with endogenous adult myosin into thick filaments and myofibrils. However, the rod interferes with normal muscle assembly resulting in cracked and frayed myofibrils that are poorly functional. In the myosin-null background, both isoforms of the headless myosin assemble into hollow thick filaments, although the lengths of these filaments are not well regulated. Myofibrils containing hexagonally packed thick filaments are also observed, but these myofibrils show irregularities in length and shape. Our results demonstrate that the myosin head is dispensable for thick filament assembly and many aspects of myofibrillogenesis, but that the interaction of the head with other myofibrillar components is likely to be required for defining the precise geometry of the sarcomere.

Results

Generation of transgenic lines expressing myosin rod isoforms

To determine the role of the myosin head in myofibrillogenesis *in vivo*, we generated two constructs that direct the expression of headless myosin molecules (Figure 1). Both constructs share the 5′ regulatory region, the first exon, the first intron and the translational start site of the *Act88F* actin gene. This region is sufficient for high levels of expression in the IFMs of the adult fly (Geyer and Fyrberg, 1986; Barthmaier and Fyrberg, 1995), the only tissue in which this gene is expressed (Hiromi and Hotta, 1985). Each construct also contains a 1.5 kb 3′ region of *Mhc*. This *Mhc* gene segment includes polyadenylation signals and was used successfully in transgenic expression of *Mhc* in *Drosophila* muscles (Hess and Bernstein, 1991; Wells *et al.*, 1996; Hodges *et al.*, 1999). Both constructs encode MHC sequence extending from 45 amino acids upstream of the head–rod junction through the C-terminus. Thus all of the globular head is missing from the expressed protein, as is part of the binding region for the essential light chain. The regulatory light-chain binding site is intact. The light-chain binding domains are inferred from their locations in the analogous chicken myosin head structure (Rayment *et al.*, 1993a,b; Bernstein and Milligan, 1997).

The two expressed rod molecules differ only in the hinge region (encoded by exon 15a or 15b) and at the C-terminus (encoded by exon 18 or 19). Construct R57-24 expresses a transcript encoding the major adult form of the myosin rod, in which exon 15a is included and in which a splicing choice is retained for exon 18 (Figure 1). Exon 18 is alternatively spliced in a stage- and tissue-specific manner (Bernstein *et al.*, 1986; Rozek and Davidson, 1986; Kazzaz and Rozek, 1989), and previous experiments demonstrated that the genomic sequence used here is sufficient for inclusion of this exon in adult *Mhc* transcripts (Hess and Bernstein, 1991). The predicted molecular mass for the encoded protein is 142 kDa. Construct R21-1 is based upon an mRNA abundant in embryonic body wall muscles (Wells *et al.*, 1996). It contains exon 15b and is prespliced at the 3′ end such that exon 18 is excluded from the mature mRNA (Figure 1, bottom), altering the amino acid sequence at the C-terminus so that it matches the embryonic isoform. The predicted molecular mass for this protein is 139 kDa.

We generated transgenic lines expressing either of these two constructs. We analyzed seven lines expressing the adult rod and nine lines expressing the embryonic rod. Lines expressing the adult rod have the prefix Y (*Y31*, *Y55-1*, *Y55-2*, *Y57*, *Y81*, *Y84* and *Y97*), whereas lines expressing the embryonic rod have the prefix V (*V18*, *V55*, *V98*, *V104*, *V115*, *V119*, *V124*, *V138* and *V143*).

Accumulation of myosin rod in a wild-type background

To determine if the truncated myosin molecules accumulate in adult muscles, we dissected the IFMs from the thoraces of young adult heterozygotes for each transgene insert and separated their constituent proteins by SDS–PAGE. We then either stained the gels with Coomassie Blue or transferred the proteins to nitrocellulose membrane for Western blotting with an anti-MHC antibody (Figure 2). By Coomassie staining, bands of apparent relative molecular mass ~130–150 kDa (labeled Rod in Figure 2A and C) accumulate in all of the transgenic lines but not in wild-type control flies. The anti-MHC polyclonal antibody recognized this ~130–150 kDa polypeptide in all of the transgenic samples (Figure 2B and D). The size of these polypeptides, their presence only in the transgenic lines and their reaction with the anti-MHC antibody demonstrate clearly that our constructs express high levels of the myosin rod. Furthermore, the rod accumulates stably in the IFMs.

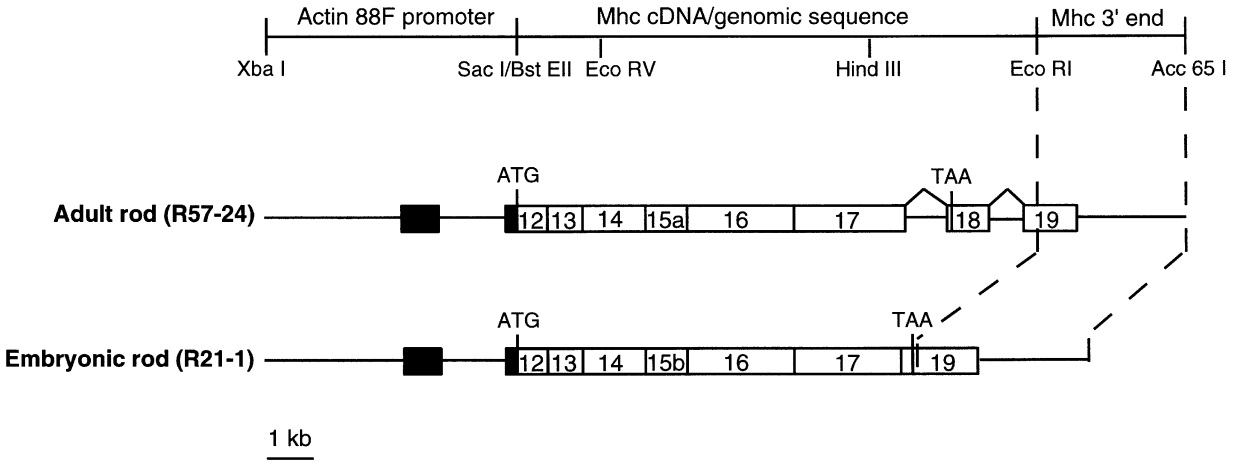

Fig. 1. Map of constructs designed to express myosin rod in indirect flight muscles. The top line shows the sources of DNA fragments and the restriction enzymes used in construction of the clones. Below are diagrams of the two constructs generated. *Act88F* exons are filled, *Mhc* exons are open. Both constructs share the *Act88F* actin gene 5′ regulatory region and promoter, and the *Mhc* 3′ end to ensure high levels of expression in adult indirect flight muscles. TAA represents the stop codons used in exons 18 (adult rod construct) and 19 (embryonic rod construct).

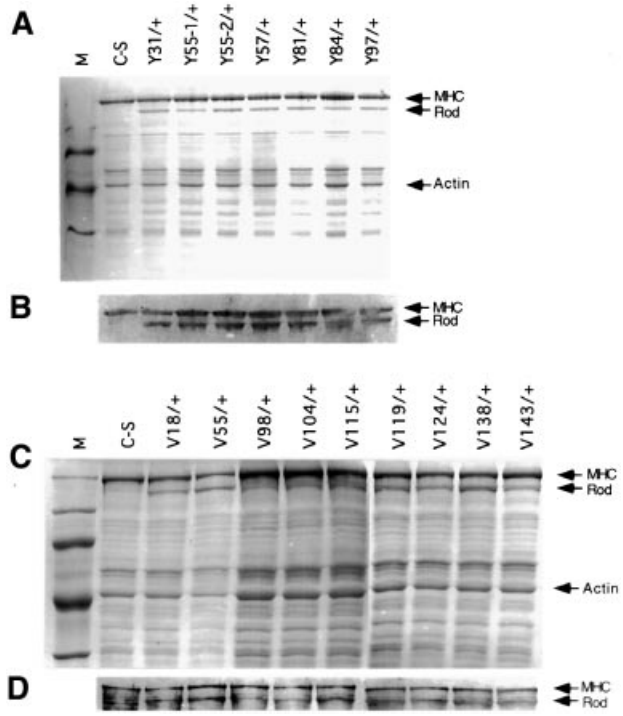

Fig. 2. All transgenic lines express the myosin rod in IFMs. SDS–PAGE of unskinned IFM proteins from lines expressing either the adult (**A**) or embryonic (**C**) isoforms of the myosin rod reveals that the rod polypeptides accumulate in the IFMs. Myosin heavy chain (MHC), actin and the ~140 kDa rod polypeptide are indicated. Anti-MHC antibody recognizes full-length MHC and the rod in Western blots of these samples (**B** and **D**). M, relative mass markers (200 kDa, 97 kDa, 68 kDa, 43 kDa, 29 kDa); C-S, Canton-S wild-type proteins.

The gels in Figure 2 suggest that each independent line expresses a distinct amount of rod protein. To quantify the levels of expression, we subjected the gels to scanning densitometry and calculated the average amounts of MHC and myosin rod relative to the levels of actin for each line (Table I). The MHC:rod ratios demonstrate that the levels of rod protein differ between the transgenic lines. We also estimated the relative accumulation of MHC molecules to rod molecules in the IFMs of different lines (see footnote to Table I). The lowest level of expression is in line *V98*/+ (~6.8:1, MHC:rod ratio) and the highest level of expression is in line *V55*/+ (~1.2:1, MHC:rod ratio). In all of the transgenic lines, the level of MHC relative to actin is slightly decreased compared with wild type, suggesting that the presence of expressed rod polypeptide influences the accumulation of full-length MHC in a minor way. In addition to studying young adults, we determined the accumulation of the rod polypeptide by SDS–PAGE during the late pupal stage in four transgenic lines. Myosin rod accumulates at similar levels relative to full-length MHC at both stages (data not shown).

To determine if the rod protein is incorporated into the IFM myofibrils, we chemically demembranated the dissected IFMs and purified the myofibrillar component after homogenization and centrifugation. Separation of these ‘skinned’ myofibrillar preparations by SDS–PAGE indicates whether the rod protein co-purifies with myofibrillar proteins under these conditions. Figure 3 shows the results for all of the adult rod lines and for two of the embryonic rod lines. Clearly, a large proportion of the rod protein remains associated with the myofibrils after demembranation, suggesting that the protein is incorporated into the myofibrillar lattice.

Antimorphic effects of myosin rod upon muscle function and myofibril assembly

To determine if expression of the rod polypeptide in the IFMs results in defects in muscle function, we flight-tested adults from each line that carries a single transgene in a wild-type background. All lines showed a reduction in flight ability compared with wild-type controls (Table I). For both the adult rod and the embryonic rod, the degree of flight impairment correlates well with the level of rod accumulation. For example, *V55*/+ accumulates the most rod protein of all of the transgenic lines and is essentially flightless; in contrast *V98*/+ shows only a slight reduction in flight ability, consistent with it expressing a much lower level of rod protein. Lines that are only mildly flight-impaired as heterozygotes are more flightless when tested as homozygotes (data not shown). These results

Table I. Expression of myosin rod in transgenic lines and effects upon flight ability

Line (chromosome)	MHC:actin ratio[a]	MHC:rod ratio[b]	MHC:rod molecules[c]	Flight ability (percentage)[d]				
				n	U	H	D	N
Adult rod								
Canton-S	2.8	–	1:0	124	79	19	1	1
Y31/+ (3)	2.5	3.4	2.1:1	117	0	0	3	97
Y55-1/+ (1)	2.5	5.2	3.2:1	73	0	29	64	7
Y55-2/+ (3)	2.5	3.2	2.0:1	85	0	0	20	80
Y57/+ (1)	2.4	3.2	2.0:1	64	0	0	2	98
Y81/+ (1)	2.4	3.6	2.2:1	89	0	0	6	94
Y84/+ (2)	2.4	7.2	4.4:1	117	32	55	11	2
Y97/+ (3)	2.4	3.5	2.1:1	113	0	0	7	93
Embryonic rod								
Canton-S	2.5	–	1:0	124	79	19	1	1
V18/+ (3)	2.2	4.6	2.9:1	102	0	0	24	76
V55/+ (3)	2.6	1.9	1.2:1	116	0	0	6	94
V98/+ (2)	2.4	10.8	6.7:1	118	52	31	16	2
V104/+ (2)	2.5	7.8	4.9:1	117	3	15	71	10
V115/+ (3)	2.4	4.5	2.8:1	106	0	0	13	87
V119/+ (3)	2.1	4.0	2.5:1	117	0	0	15	85
V124/+ (3)	1.9	3.6	2.2:1	120	0	0	3	98
V138/+ (3)	2.2	2.5	1.5:1	114	0	0	4	96
V143/+ (3)	2.5	5.6	3.5:1	108	17	15	15	54

[a]Levels of myosin heavy-chain, myosin rod and actin were determined by scanning densitometry and expressed in arbitrary units; all samples were then normalized based on the levels of actin in each lane and the MHC:actin ratio was determined.
[b]For the myosin rod, normalized levels of rod protein in the transgenic lines were calculated as described above. The normalized reading obtained from the same region of the gel in the Canton-S sample (where no rod protein is expressed) was subtracted from the levels of rod, to compensate for background signal. MHC:rod ratios were then determined. By definition the level in the Canton-S sample is zero.
[c]The MHC:rod molecular ratio was determined after assuming that the affinities for Coomassie stain were similar for MHC and for the rod. The number of MHC molecules relative to each rod was determined by dividing the level of MHC (in arbitrary units) by the ratio of the calculated relative molecular masses of MHC:rod (1.64 for the adult rod and 1.60 for the embryonic rod) prior to calculating the MHC:rod ratio.
[d]Flight ability was determined as described in Materials and methods: U, upward flight; H, horizontal flight; D, downward flight; N, no flight.
n, number tested.

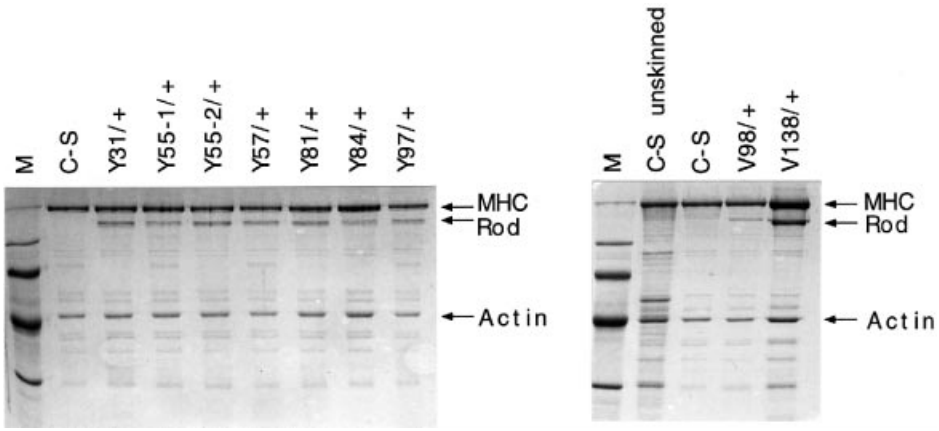

Fig. 3. The myosin rod molecules are associated with the myofibrillar fraction of chemically demembranated muscles. Left panel shows IFM proteins of lines expressing the adult rod. Right panel shows IFM proteins of unskinned and skinned wild-type Canton-S (C-S), and two representative lines expressing the embryonic rod. M, relative mass markers (200 kDa, 97 kDa, 68 kDa, 43 kDa, 29 kDa).

demonstrate that the expressed rod molecules interfere with flight muscle function.

Comparisons of lines expressing different constructs but with similar levels of rod protein accumulation demonstrate that the embryonic rod has a more severe effect upon flight ability than the adult rod. Lines *V104*/+ and *Y84*/+ have similar levels of expression, yet 81% of *V104*/+ fly either Down (D) or Not-at-all (N) whereas only 13% of *Y84*/+ fly in a similar manner (Table I). Similar conclusions can be drawn by comparing lines *V143*/+ and *Y55-1*/+. Thus the embryonic and adult rods display isoform-specific properties.

To determine the effects upon myofibrillogenesis of expression of headless myosin molecules, we studied pupal IFMs from representative lines by transmission electron microscopy. We used pupal samples to ensure that any observed defects are due to abnormal assembly rather than to use- or time-dependent degeneration, as has

been observed in some other mutants (Fyrberg *et al.*, 1990; Beall and Fyrberg, 1991; Kronert *et al.*, 1995; Wells *et al.*, 1996).

Electron microscopy revealed that thick filaments and myofibrils assemble when rod molecules are co-expressed with endogenous wild-type MHC, but that the myofibrils are structurally defective (Figure 4). In wild-type pupal IFMs, the hollow thick filaments are arranged in a regular hexagonal manner, and thin filaments are interdigitated between the thick filaments (Figure 4A and B). In lines expressing each of the rod isoforms, sarcomeres form although frequent cracks occur in the myofilament lattice; sarcomere length and width are more variable than in wild-type (Figure 4C and E). In transverse section, hollow thick filaments accumulate and most of these are assembled into hexagonally packed arrays of myofilaments. However, there are clear defects in the packing of these filaments and the myofibrils are frequently not round in cross-section (Figure 4D and F).

To quantify the phenotypic effects of expressing the myosin rod in a wild-type background, we measured sarcomere lengths, myofibril diameters and the number of thick filaments per μm^2 for wild type and a line expressing each of the transgenes (Table II). While average sarcomere length is not affected by the adult rod, expression of the embryonic rod significantly decreases the sarcomere length ($p < 0.05$ by Student's *t* test). Most notably the variability of the sarcomere length, as shown by the standard error values, is increased by 25–85% as a result of transgene expression. Sarcomere length variability directly reflects increased variability in thick filament length, since thick filaments extend nearly the entire length of the sarcomere in insect IFMs. Myofibril diameter is increased by ~20% (statistically significant differences) as a result of expression of either transgene in a wild-type background and the variability increases 2- to 3-fold. Transgene expression yields a statistically significant reduction (~40%) in the number of thick filaments per cross-sectional area.

Our data demonstrate that headless myosin does not prevent the assembly of the endogenous wild-type MHC into thick filaments but that headless molecules interfere with the higher-ordered assembly of myofibrils. Resulting defects in flight ability occur even at very low levels of transgene expression. These phenotypes do not arise simply from increased protein accumulation, since doubling of the *Mhc* gene dosage is necessary for IFM defects and flight impairment to occur (Cripps *et al.*, 1994). We conclude that the expressed rod molecules interfere with myofibril assembly and function in a wild-type background.

Assembly of myosin molecules

Based on the *in vivo* accumulation of the myosin rod molecules and their association with the myofibrillar protein fraction, the rods appear to assemble with the endogenous myosin into the myofibrils. We therefore determined whether the rod molecules form heterodimers with full-length MHC *in vivo*. We purified native IFM myosin from wild-type, from lines expressing the adult or embryonic rods in a wild-type background, and from lines expressing the rod molecules in an Mhc^{10} mutant background that lacks MHC in the IFM (Collier *et al.*, 1990). SDS–PAGE of the purified myosin is shown in Figure 5, top panel. Both full-length MHC and myosin rod are visible in these preparations, demonstrating that the rod can be purified using this method, even in the absence of endogenous MHC. Smaller bands likely correspond to MLC2 (myosin light chain 2 or regulatory light chain) and the MLCA (alkali myosin light chain or essential light chain).

Under native conditions, myosin from Canton-S wild-type flies migrates as a single band, designated complex 1, corresponding to the native hexameric myosin molecule (Figure 5, bottom two panels). Myosin rod expressed in an MHC-null background also forms a single band, designated complex 3, which migrates more quickly than complex 1. The protein in complex 3 is likely to be a homodimer of the rod molecule for the following reasons: (i) it has similar solubility properties to full-length native myosin; (ii) it can assemble into thick filaments and myofibrils when expressed in an MHC-null background (see following section); (iii) previous *in vivo* studies showed that myosin rods form homodimeric molecules in *Drosophila* muscles (Standiford *et al.*, 1997).

In myosin prepared from muscles in which the rod and full-length MHC are co-expressed, complexes 1 and 3 are the major bands observed, indicating that the majority of the myosin rod expressed in the IFMs exists as a homodimer. A much fainter band with intermediate mobility (complex 2) is observed consistently. Its migration pattern suggests that complex 2 represents a heterodimer of full-length MHC with the rod molecule. Analyses of bands excised from the gel and re-electrophoresed under denaturing conditions are consistent with this conclusion (data not shown).

Assembly of myosin rod in a myosin-null background

To determine whether thick filament and myofibril assembly are dependent upon the presence of the myosin head, we analyzed flies expressing myosin rods in an Mhc^{10} mutant background. In Mhc^{10} control flies, arrays of thin filaments and malformed Z-discs accumulate in IFMs; however, no thick filaments form since MHC is not produced in these muscles (Collier *et al.*, 1990; Cripps *et al.*, 1994; Figure 6A and B). In contrast, rod molecules clearly are capable of assembly into higher-ordered structures, since they can be purified as high salt extracts from skinned IFMs (Figure 3).

In Mhc^{10} flies expressing the adult rod (*w; Mhc^{10}; Y97*), longitudinal sections reveal the presence of thick filaments that are associated into myofibril-like structures (Figure 6C). These myofibrils have Z-discs and occasional M-lines; however, sarcomere length is variable, as is the length of the thick filaments. The Z-discs are thicker than in wild-type, suggesting that they do not form normally, or lose integrity after assembly. In transverse section (Figure 6D), all of the thick filaments show hollow centers, a characteristic of IFM thick filaments. In addition, many of these filaments are packed in a hexagonal manner and frequently are interdigitated with thin filaments. Often, six thin filaments surround each thick filament, as in wild type. However, the myofibrils are rarely circular in cross-section and show a variability in size compared with the regularity found in normal IFM.

In lines expressing the embryonic rod in an Mhc^{10}

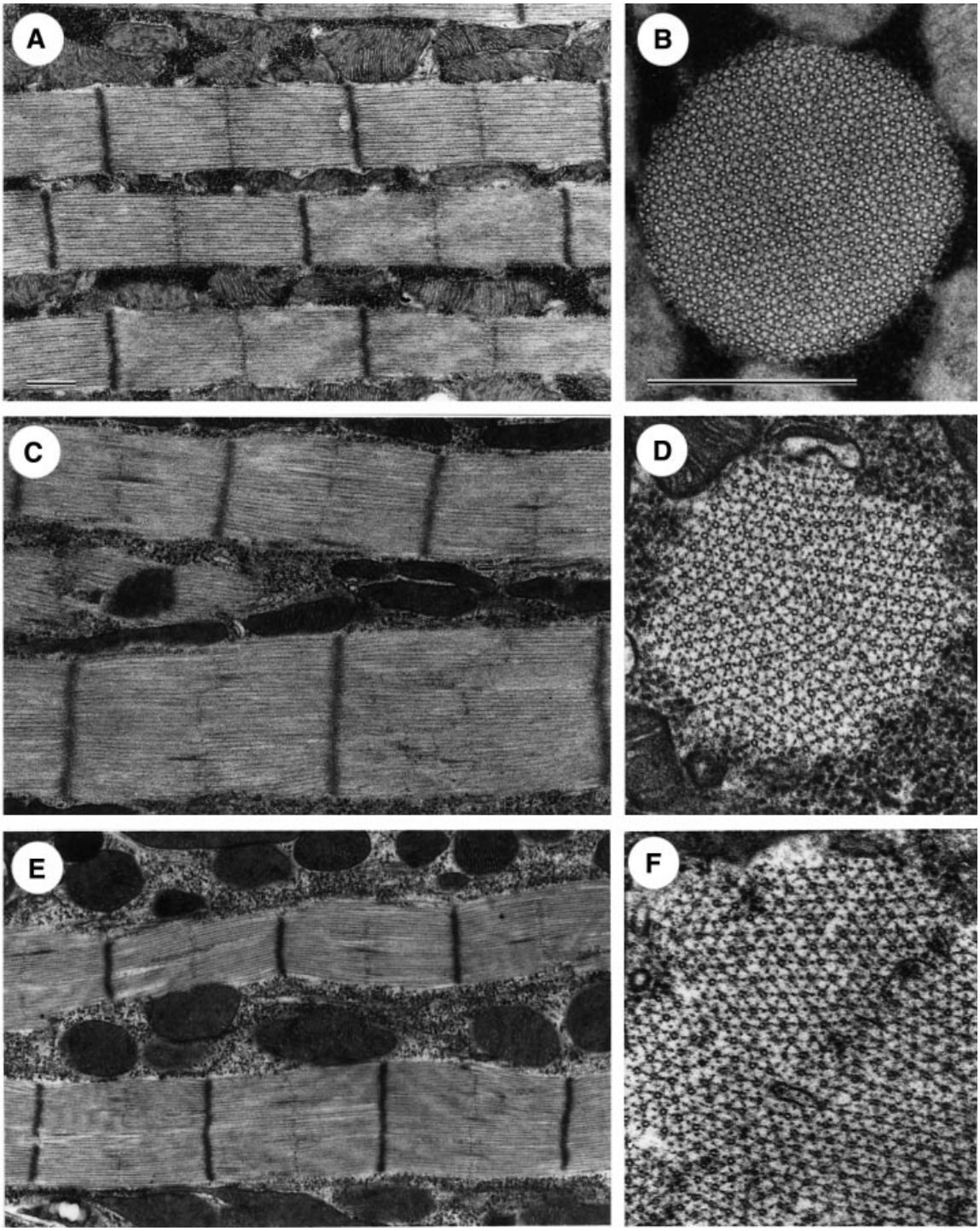

Fig. 4. Expression of myosin rod in a wild-type background causes defects in myofibril assembly. (**A**) Wild-type, longitudinal section. Sarcomeres of regular width and length are separated by darkly stained Z-lines and bisected by M-lines. (**B**) Wild-type, transverse section. Hollow thick filaments are packed in a hexagonal array; each is surrounded by six thin filaments. (**C**) Adult rod transgene (*Y97*/+) expressed in a wild-type background, longitudinal section. Cracks in the sarcomere lattice and irregularities in sarcomere length and diameter occur. M-lines are disrupted. (**D**) *Y97*/+ transverse section. Filament packing is less uniform than wild type with irregular myofibril border. (**E**) Embryonic rod transgene (*V138*/+) expressed in a wild-type background, longitudinal section. Cracks and irregularities in myofibril diameter are evident. (**F**) *V138*/+ transverse section. Filament packing is disrupted and interfilament distance is noticeably increased compared with wild type. All samples are of late pupal IFMs. Bars, 0.5 μm.

background (*w; Mhc^{10}; V138*), hollow thick filaments and myofibril-like structures are also formed, although to a lesser extent (Figure 6E and F). Hexagonal packing of thick filaments is observed in transverse sections with arrays of six thin filaments surrounding each thick filament (Figure 6F). This also is limited to smaller localizations. As expected, neither adult nor embryonic rod molecules rescue flight in the *Mhc^{10}* background, proving that the myosin head is required for muscle function.

Quantitative analysis (Table II) shows that the sarcomere

Table II. Effects of myosin rod expression on myofibril dimensions

Genotype	Stage	Sarcomere length (μm)	Myofibril diameter (μm)	Thick filaments/μm^2
w^{1118}: wild type (wt)	pupal	2.64 ± 0.018 (51)	0.813 ± 0.026 (20)	1115.6 ± 17.9 (20)
Y97/+: adult rod, wt background	pupal	2.64 ± 0.033 (56)	0.978 ± 0.088 (20)	675.7 ± 12.9 (20)
V138/+: embryonic rod, wt background	pupal	2.29 ± 0.022 (53)	0.969 ± 0.053 (23)	727.3 ± 25.4 (23)
w^{1118}: wild type	young adult	3.31 ± 0.017 (55)	1.006 ± 0.011 (20)	938.3 ± 16.1 (20)
Mhc^{10}: MHC null	young adult	0.99 ± 0.047 (57)	ND[a]	0
Mhc^{10};*Y97*: adult rod, MHC null background	young adult	2.20 ± 0.086 (49)	ND	792.4 ± 24.9 (21)
Mhc^{10};*V138*: embryonic rod, MHC null background	young adult	2.01 ± 0.096 (48)	ND	560.8 ± 21.8 (21)

Mean values are given ± the standard error of the mean. Number of samples measured is given in parentheses.
[a]ND, not determined due to the irregular shape of myofibrils.

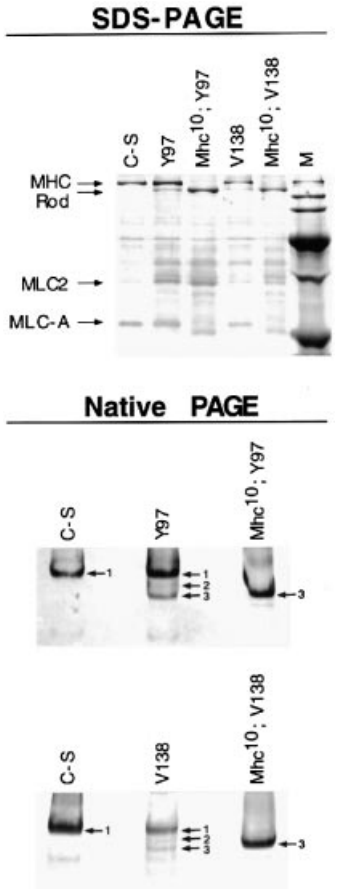

Fig. 5. Analysis of myosin subunit structure by native gel electrophoresis. Top: SDS–polyacrylamide gel stained with Coomassie Blue to show the purified myosins. The positions of MHC, rod, MLC2, the regulatory light chain and MLCA, the essential light chain are indicated. Myosin from lines expressing the rod in the Mhc^{10} background contains MLC2 but not MLCA. M, relative mass markers (200 kDa, 97 kDa, 68 kDa, 43 kDa, 29 kDa, 18 kDa); C-S, Canton-S wild type. Center and bottom: native polyacrylamide gel stained with Coomassie Blue to determine myosin subunit structure. Complexes detected are: 1, homodimer of full-length MHC; 2, heterodimer of MHC and rod; 3, homodimer of rod. There is little formation of heterodimers of rod and full-length MHC when either the adult rod (center; *Y97*) or embryonic rod (bottom; *V138*) is co-expressed with wild-type myosin.

lengths of myofibrils containing either the embryonic or the adult rod are significantly (~30%) shorter and several-fold more variable than in wild type ($p < 0.05$). Interesttingly, the length of the sarcomeres is significantly longer in the transgenics compared with myosin-null IFMs, indicating that thick filaments are important in dictating this property. Due to the irregularity of the myofibrils in cross-section, it was not possible to determine their average diameter. However, the number of thick filaments per μm^2 is significantly smaller in the transgenics (~30%) than in wild-type adults.

While both isoforms of the rod are capable of producing hollow thick filaments that interdigitate appropriately with thin filaments, the adult rod is superior in restoring sarcomeric structure (Figure 6) and thick filament packing density (Table II). Overall, our results clearly demonstrate that many aspects of thick filament assembly and myofibrillogenesis can proceed *in vivo* in the absence of the myosin head.

Discussion

Thick filaments of insect IFMs are characteristically hollow in cross-section and are packed into myofibrils in a hexagonal arrangement. Thin filaments interdigitate so that six of them surround each thick filament. This precisely ordered array is likely to be a requirement for the novel mechanical properties of insect IFMs (Wray, 1979). The mechanism by which the macromolecular assembly of muscle proteins is orchestrated in this muscle, or in other muscles, is largely unknown.

Here, we determined if the globular head of the myosin molecule is required in a muscle cell for thick filament assembly. We find that headless myosin molecules can assemble into filaments in the IFM of *Drosophila melanogaster*, and that they display the hollow cross-section characteristically found in this muscle type. While earlier studies showed that headless myosins can assemble into higher order structures *in vitro* (Lowey *et al.*, 1969; Nyitray *et al.*, 1983; Sohn *et al.*, 1997), ours is the first such demonstration within a muscle cell. Our results contrast with evidence that the function of the head is required for filament formation in *C.elegans* body wall muscles (Bejsovec and Anderson, 1988, 1990), and possibly in *Drosophila* IFM (Kronert *et al.*, 1994). Also in apparent disparity with the *C.elegans* data, we find that the presence of headless myosin in muscle cells does not interfere dramatically with the accumulation of endogenous MHC. We propose two explanations for these differences. One is that the *C.elegans* mutations do not simply inactivate ATPase activity or actin-binding functions of the mutant MHCs but instead induce novel interactions that prevent thick filament assembly. Alternatively, there

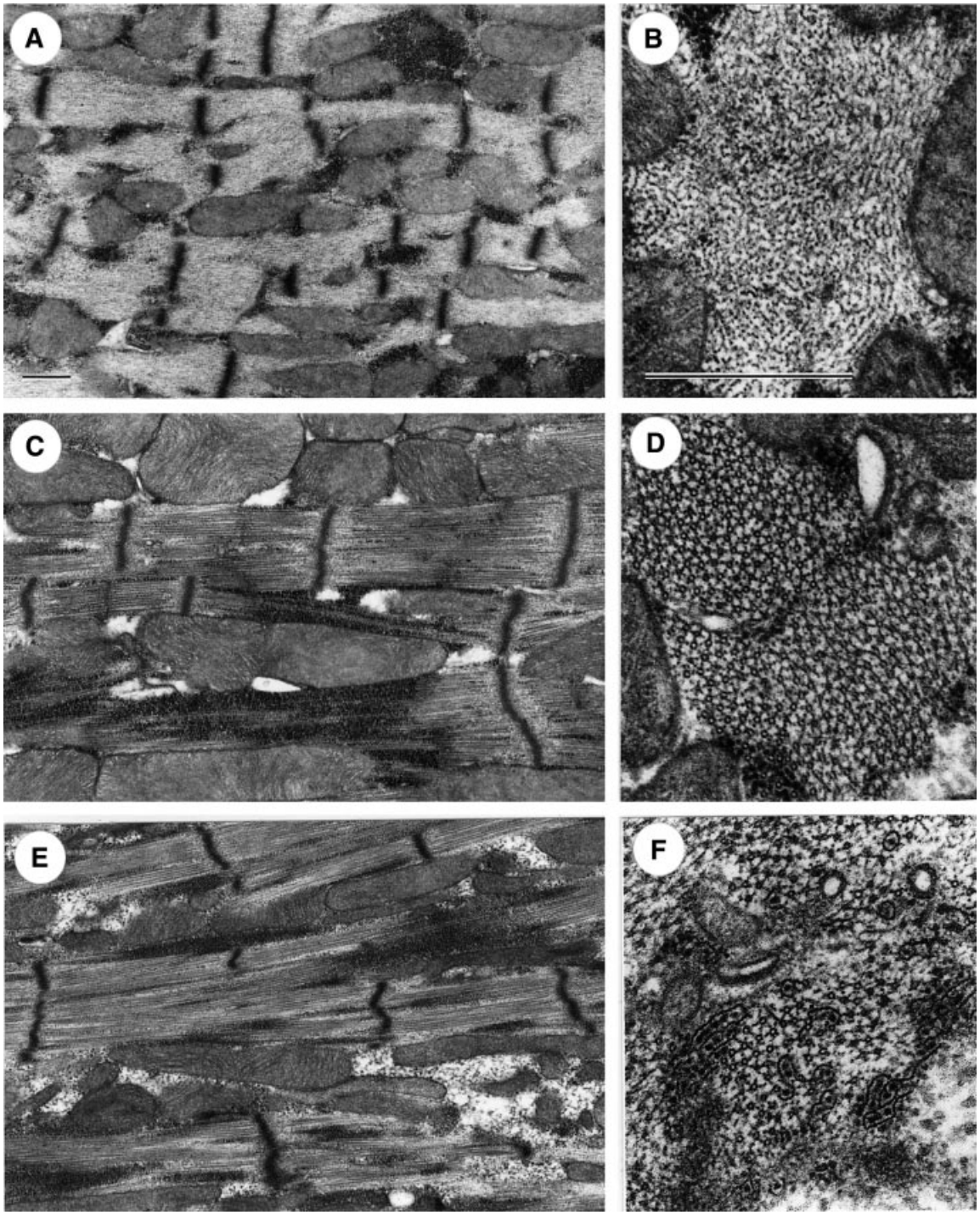

Fig. 6. Headless myosin assembles into IFM thick filaments and myofibrils in an MHC null background. (**A**) and (**B**) Phenotype of *Mhc*^{10} mutants. A longitudinal section (A) of IFM from the *Mhc*^{10} mutant shows skeins of thin filaments that accumulate with Z-body material. In transverse section (B) no thick filaments are present. (**C**) and (**D**) Homozygotes for the adult rod isoform transgene (*Y97*) in *Mhc*^{10} mutants. In longitudinal section (C) numerous thick filaments associate into myofibril-like structures, although thick filament length is highly variable, as is sarcomere length and width. In transverse section (D) thick filaments are clearly hollow and are packed in a roughly hexagonal manner. They frequently interdigitate with thin filaments so that six thin filaments surround each thick. (**E**) and (**F**) Homozygotes for the embryonic rod transgene (*V138*) in *Mhc*^{10} mutants. Longitudinal section (E) reveals that filaments also form myofibril-like structures, although to a lesser extent than adult rod filaments. In transverse section (F) thick filaments are generally hollow and are commonly packed in a manner similar to wild type. Some electron-dense thick filaments are present and these are surrounded by dense thread-like structures of unknown origin. All samples are of young adult IFMs. Bars, 0.5 μm.

may be fundamental differences in the mechanisms of thick filament assembly between *C.elegans* and *Drosophila*. This may reflect different roles of myosin-associated proteins in the two species.

Our data indicate that thick filaments assembled *in vivo* from headless myosins are capable of co-assembly with thin filaments into myofibrils. Many thick filaments are packed in a hexagonal manner and there is the normal arrangement of six thin filaments surrounding each thick filament. Thus, despite the presence of known sites of

actin interaction in the myosin head, proper organization and interdigitation of myofilaments do not require this portion of the myosin molecule. Since re-assembly of myofibrils from constituent proteins has not been achieved *in vitro*, our study represents the first demonstration that a specific domain of the myosin molecule is dispensable for many aspects of myofibril assembly. The regions of the myosin rod required for higher order assembly can be dissected eventually using the *Drosophila* model system.

Despite the regulated assembly of headless myosin molecules into the myofibrillar lattice, the presence of the myosin head appears to be required for completely normal sarcomere structure. When the myosin rod is expressed in a wild-type background, sarcomere fraying, lack of uniformity in thick filament and sarcomere lengths, irregularity in myofibril diameters and thick filament spacing, myofibril cracking and loss of flight ability occur. These defects are unlikely to result simply from inappropriate levels of expression of myosin relative to other sarcomeric components. Reductions in flight ability are observed in this study even at very low levels of expression of the transgene in a wild-type background, whereas previous studies demonstrated that severe flight abnormalities require that the *Mhc* gene dosage be doubled (Cripps *et al.*, 1994). Furthermore, the phenotypes we observe are different compared with the defects observed when MHC is overexpressed: in this study the myofibrils show cracks and disruptions to the hexagonal packing throughout their lengths and diameters, whereas defects caused by overexpression are limited to the periphery of the myofibrils (Cripps *et al.*, 1994). We also determined directly if reducing endogenous MHC levels to compensate for the amount of rod protein present could rescue the flight defects observed. We crossed lines expressing the rod molecules to homozygous Mhc^{10} flies to generate $Mhc^{10}/+$ individuals containing one copy of the transgene. In no case was there rescue of flight ability (our unpublished observations), suggesting that the flight defects observed are not related to overexpression of myosin.

The importance of the myosin head to myofibril assembly is most dramatically demonstrated by the variability in length and shape of sarcomeres formed from myosin rod expression in the MHC-null background. Again, it does not appear that these effects arise from inappropriate levels of rod expression, since we chose to study lines in which the accumulation of myosin rod was close to levels expected for intact MHC (see Table I).

An alternative possibility to explain myofibril assembly defects arising from rod accumulation is an inappropriate time of expression of the transgenes. The *Act88F* promoter used in this study is active at 16 h of pupariation, ~10 h prior to the wild-type *Mhc* promoter (Fernandes *et al.*, 1991). However, it is unlikely that this explains all of the abnormalities in muscle development, since there is no evidence for myofibril assembly in wild-type IFMs during these early hours of development; thick and thin filaments are not observed until ~38 h of pupariation at 25°C (42 h at 22°C; Reedy and Beall, 1993).

The likely explanation for the myofibril assembly defects we observe is that headless myosin is deficient in its interactions with other components of the sarcomere. Numerous proteins are implicated in the regulation of muscle assembly, including the myosin-binding proteins titin, myomesin, C-protein and H-protein (reviewed in Epstein and Fischman, 1991; Vikstrom *et al.*, 1997). H-protein and C-protein organize myosin filaments generated in non-muscle cells (Seiler *et al.*, 1996), and the myosin rod binds to C-protein (Moos *et al.*, 1975) and myomesin (Obermann *et al.*, 1997) *in vitro*. Although the major interaction of titin is with the myosin rod (Houmeida *et al.*, 1995), there is also evidence that titin interacts with the myosin head (Wang *et al.*, 1992). None of these proteins, except for titin (Machado *et al.*, 1998) and a titin analog named projectin (Ayme-Southgate *et al.*, 1991; Fyrberg *et al.*, 1992), has been found in *Drosophila*. In insect IFM, a tropomyosin isoform named troponin-H has a C-terminal extension that contacts the myosin cross-bridge (Reedy *et al.*, 1994), and the thick filament-associated protein flightin might also play a role in muscle assembly (Vigoreaux *et al.*, 1998). Interactions between the myosin rod and some of these factors are likely to be normal in the absence of the myosin head, permitting interdigitation of thick and thin filaments. However, interaction of the myosin head with such proteins may be required to regulate sarcomere growth during development, yielding the defects we observe when the head is absent.

We demonstrated that when myosin rod and full-length myosin are co-expressed in the IFM there is little heterodimer formation to generate single-headed myosin molecules. While it is possible that heterodimers formed but were not efficiently purified by high salt extraction, this seems unlikely since homodimers of both full-length myosin and of myosin rod were efficiently extracted using standard procedures. Our observations contrast with those of Burns *et al.* (1995) who expressed myosin rod in *Dictyostelium discoideum*, and found that the rod molecules rarely formed homodimers and instead were associated predominantly with endogenous full-length myosin as heterodimers. They hypothesized that this was due to heterodimer formation occurring much more quickly than the formation of rod homodimers in these cells. One possible explanation for these differences might be that myosin molecules are rapidly sequestered into thick filaments and myofibrils during IFM development, whereas the cytoplasmic myosin in *D.discoideum* may remain cytosolic for some time. It is possible that the rapid assembly of *Drosophila* components into muscles either stabilizes or promotes the formation of the rod homodimer.

In agreement with our observation that myosin–rod heterodimers rarely form, Standiford *et al.* (1997) recently reported that a naturally occurring myosin rod protein (MRP) accumulates as a homodimer in a number of *Drosophila* muscle types (it is not present in IFM). This protein contains a unique N-terminal extension, and forms mixed filaments with standard myosin. Standiford *et al.* (1997) propose that MRP reduces the maximal power output of muscles in which it is expressed since MRP would not be capable of forming cross-bridges with thin filaments. Direct flight muscles containing MRP have thin filaments that 'wander' from their thick filament partner, probably because of the absence of some cross-bridges. In support of observations and hypotheses regarding MRP, our data demonstrate that myosin lacking its globular head can have disruptive effects upon myofibril structure and function.

Both embryonic and adult rod isoforms disrupt wild-type IFM assembly and physiology. Further, each isoform can assemble into thick filaments and myofibrillar structures in the absence of endogenous myosin. The identity of the MHC isoform does not influence the thin filament orbital number, a property that differs between embryonic muscle and IFM (Wells *et al.*, 1996). However, there are also isoform-specific properties displayed by the embryonic and adult rods: the embryonic isoform is more antimorphic to wild-type myosin function and rescues thick filament and myofibril structure less well than the adult rod. Thus the two isoforms are not completely interchangeable. This is consistent with our earlier study demonstrating that adult and embryonic MHCs display isoform-specific properties in stabilizing myofibril structure (Wells *et al.*, 1996). In our current work, the phenotypic differences resulting from expression of the two rod proteins must result from variations in the hinges and/or C-termini, the only areas that differ between the isoforms.

In summary, we demonstrated that the myosin head is not required *in vivo* for assembly of the thick filament, nor for initial ordered association of these filaments into a mature myofibril. However, the myosin head is required to properly regulate the morphology of the sarcomere. We obtained these results using a model system in which the mechanisms of myofibril assembly can be dissected readily in intact muscles *in vivo*, and where muscle function is not required for viability of the organism. We anticipate that this system will prove valuable in the future for identifying functional domains of known contractile proteins and novel factors that are essential to myofibrillogenesis.

Materials and methods

Generation and transformation of constructs expressing the myosin rod

To produce a fusion of the *Act88F* promoter and translational start site with the *Mhc* cDNA expressing the embryonic form of the myosin rod (Figure 1), we first generated a PCR product containing the *Act88F* promoter and ~2 kb of 5′ upstream sequence; the 3′ primer (sequence 5′-GCGCGAGCTCCATCTTGGCAGTTGTTTATCTGG-3′) yielded a unique *Sac*I site immediately after the ATG initiation codon. This fragment was cloned into pBluescript II KS (pKS, Stratagene) as an *Xba*I–*Sac*I fragment. This plasmid, pL116-4, was then cut at the *Sac*I site and the protruding end was removed with mung bean nuclease (New England Biolabs). The plasmid was then cleaved with *Xba*I to release the promoter fragment and translational start site.

To generate a cDNA fragment corresponding to the embryonic myosin rod, a full-length embryonic cDNA cloned in pKS (Wells *et al.*, 1996) was cleaved at a *Bst*EII site in exon 12, which corresponds to 45 amino acids upstream of the head–rod junction in the protein. The *Bst*EII protruding end was filled-in using Klenow fragment (New England Biolabs) and this DNA was then cut with *Xba*I to release the head-coding sequences and to allow insertion of the *Act88F* promoter fragment isolated above as an *Xba*I blunt-ended insert. Ligation of the treated *Sac*I site to the filled-in *Bst*EII site resulted in an in-frame fusion of the *Act88F* promoter and ATG codon to the *Mhc* cDNA sequence. The fusion regenerated the *Bst*EII site and was confirmed by sequencing. All other cloning steps used standard procedures (Sambrook *et al.*, 1989) making use of the restriction sites shown in Figure 1. The completed construct encoding the embryonic rod is designated R21-1.

The adult rod construct, R57-24, was constructed using R21-1; we switched the exon 15 region by replacing the *Eco*RV–*Hin*dIII fragment with the similar fragment from cD301 (George *et al.*, 1989). The C-terminus was switched as an *Hin*dIII–*Eco*RI fragment to remove the pre-spliced exons 17–19 and replace them with a genomic fragment retaining the normal exon 17-18-19 structure with introns. We showed (Hess and Bernstein, 1991) that this fragment is sufficient to carry out the correct stage- and tissue-specific splicing of exon 18 observed for the endogenous *Mhc* gene (Bernstein *et al.*, 1986; Rozek and Davidson, 1986).

We cloned each construct into a P-element transformation vector, pCaSpeR K [a modified form of pCaSpeR that contains a unique *Kpn*I (*Acc*65I) site in place of the unique *Eco*RI site]. Germline transformation was performed essentially as described by Rubin and Spradling (1982), using the helper plasmid delta2-3 (Robertson *et al.*, 1988). Embryos of the genotype w^{1118} were injected and potential transformants were recovered in the G_1 generation as orange-eyed individuals. Transformed lines were mapped and made homozygous by standard crosses. Linkage group analysis was performed using *w; SM1/Sco; TM2/MKRS*, and this stock was also used to cross some of the transformed lines into the Mhc^{10} background.

Fly culture

Gene and chromosome symbols are as described by Lindsley and Zimm (1992). Flies were grown on Carpenter's medium (Carpenter, 1950) either in 100×25 mm glass vials or in half-pint milk bottles at 25°C.

Flight testing

Flight testing was performed as described by Drummond *et al.* (1991), upon 1- to 2-day-old flies. Briefly, flies were released inside a clear plastic box illuminated from the top. Flies were scored for whether they flew Upward toward the light (U), Horizontally (H), Downward but still with some small flight ability (D) or Not-at-all (N).

Protein preparation and electrophoresis under denaturing conditions

SDS–PAGE was performed as described by Laemmli (1970), using a Bio-Rad Mini-Protean II minigel apparatus. Gels were stained with Coomassie Blue R-250 and dried in cellophane. Protein levels were quantified by scanning densitometry using a Molecular Dynamics densitometer model PD. Myosin and rod levels were quantified relative to actin, and all results are the average of scans from two separate gels.

For unskinned samples of IFM proteins, the dorsal longitudinal muscles (DLMs) from two to four flies were dissected from the thorax as described by Peckham *et al.* (1990) and homogenized in 60 µl of SDS–PAGE sample buffer; the equivalent of the protein from the DLMs of a quarter of a fly were loaded per lane. Some IFM samples were chemically demembranated (skinned) following the protocol of Cripps and Sparrow (1992); the equivalent of the DLMs from half a fly were loaded in each lane of the gel.

Western blotting

Western blotting was performed essentially as described by Sambrook *et al.* (1989). Briefly, proteins were transferred from SDS–polyacrylamide gels to nitrocellulose membrane using a semi-dry blotting apparatus (American Bionetics, Inc.). Myosin polypeptides were detected using a 1:500 dilution of rabbit anti-*Drosophila* MHC polyclonal antibody (Kiehart and Feghali, 1986) and an alkaline phosphatase-linked goat anti-rabbit secondary antibody diluted to 1:1000 (Bio-Rad). Localized alkaline phosphatase activity was detected using nitro-blue tetrazolium and X-phosphate (Boehringer Mannheim).

Purification of native myosin

Myosin was purified from 10–20 young adult flies as previously described (Kronert *et al.*, 1995), with minor modifications. Briefly, the IFMs were dissected from flies in York Modified Glycerol (YMG; Peckham *et al.*, 1990) and homogenized in this buffer. After centrifugation at 14 000 *g* for 5 min at 4°C, the supernatant was removed and the pelleted myofibrils were washed once with 100 µl of YMG. They were then pelleted as above. Myofibrils were washed with 100 µl of relaxing solution (Peckham *et al.*, 1990) and pelleted as before; the aim of this step was to release any myosin heads which were bound to actin filaments, thereby reducing the amount of actin that was co-purified with myosin. Myosin was extracted from the pellet in 25 µl of high salt buffer (800 mM KCl, 50 mM potassium phosphate buffer pH 7.0, 1 mM dithiothreitol) for 5 min on ice. Undissolved myofibrillar material was pelleted at 14 000 *g* for 5 min at 4°C, and the supernatant containing the myosin was carefully removed to a fresh tube. Myosin was then precipitated by the addition of 250 µl of cold water, and this mixture was left overnight on ice. Myosin was pelleted at 14 000 *g* for 15 min at 4°C, and the supernatant was discarded. The myosin pellet was resuspended in 20 µl of myosin storage buffer [Butler-Browne and Whalen, 1984; 40 mM sodium pyrophosphate, 50% (v/v) glycerol pH 8.5] and stored at –20°C. Typically, 2 µl of this preparation was

used for visualization by SDS–PAGE and 8–10 μl for electrophoresis under native conditions.

Electrophoresis under native conditions

Native PAGE of purified myosins was essentially as described by Butler-Browne and Whalen (1984), except that higher concentrations of ammonium persulfate and *N*,*N*,*N*',*N*'-tetramethyl ethylenediamine were used (d'Albis *et al*., 1979); β-mercaptoethanol was also included in the running buffer at a final concentration of 1.4 mM (Whalen *et al*., 1981). Electrophoresis of native gels was performed in a Bio-Rad Mini-Protean II minigel apparatus for 3 h at 50 V and at 4°C. Gels were stained with Coomassie Blue R-250 and destained. They were photographed wet.

Electron microscopy

For electron microscopy of pupal samples, pupae within 12 h of eclosion were collected. Thoraces were isolated using a double-edged razor blade to remove anterior and posterior tissues. For samples of young adult flies, thoraces were isolated using a double-edged razor blade to remove the head, abdomen and a ventral portion of the thorax. Tissues were fixed overnight and then post-fixed. Following dehydration with acetone, samples were embedded in EMbed-812 resin (Electron Microscopy Sciences). Samples were infiltrated with resin by first placing them in a mixture of 50% resin/50% acetone (v/v) for at least 3 h. This was replaced with a 75% resin/25% acetone (v/v) mixture and left overnight. The following day, samples were transferred into 100% resin for several hours, then put in embedding molds with fresh resin and placed under vacuum for 3 h. Samples were oriented within the molds and polymerized at 60°C under vacuum overnight. Other details of sample preparation and observation were according to O'Donnell and Bernstein (1988).

We quantified myofibril defects by measuring micrographs of transverse and longitudinal sections of IFMs. The former were used to determine myofibril diameter and thick filaments per square micron, and the latter to determine sarcomere length. Mean values and standard errors were calculated using data from multiple samples. Student's *t*-tests were performed to determine whether mean value differences are statistically significant ($p < 0.05$).

Acknowledgements

We are very grateful to John Sparrow for invaluable assistance with IFM dissections, to Sarah Montross for excellent laboratory support and to Henry Epstein for valuable discussions in the early stages of this work. We thank Mary B.Davis and Charles Emerson,Jr for providing the cD301 cDNA clone, Eric Fyrberg for the *Actin88F* genomic clone and Daniel Kiehart for the myosin antibody. We are grateful to Steve Barlow for advice on electron microscopy, which was performed in the San Diego State University Electron Microscope Facility. We appreciate critical comments on the manuscript provided by Douglas Swank, Michelle Mardahl-Dumesnil and William Kronert and help with the statistical analysis from Douglas Swank. This research was supported by grants GM32443 and AR43396 from the NIH to S.I.B.

References

d'Albis,A., Pantaloni,C. and Bechet,J.-J. (1979) An electrophoretic study of native myosin isozymes and of their subunit composition. *Eur. J. Biochem*., **99**, 261–272.

Ayme-Southgate,A., Vigoreaux,J., Benian,G. and Pardue,M.L. (1991) *Drosophila* has a twitchin/titin-related gene that appears to encode projectin. *Proc. Natl Acad. Sci. USA*, **88**, 7973–7977.

Bandman,E.M., Arrizubieta,J., Wick,M., Hattori,A., Tablin,F., Zhang,S. and Zhang,Q. (1997) Functional analysis of the chicken sarcomeric myosin rod: regulation of dimerization, solubility, and fibrillogenesis. *Cell Struct. Funct.*, **22**, 131–137.

Barthmaier,P. and Fyrberg,E. (1995) Monitoring development and pathology of *Drosophila* indirect flight muscles using green fluorescent protein. *Dev. Biol.*, **169**, 770–774.

Beall,C.J. and Fyrberg,E.A. (1991) Muscle abnormalities in *Drosophila melanogaster* heldup mutants are caused by missing or aberrant troponin-I isoforms. *J. Cell Biol.*, **114**, 941–951.

Bejsovec,A. and Anderson,P. (1988) Myosin heavy-chain mutations that disrupt *Caenorhabditis elegans* thick filament assembly. *Genes Dev.*, **2**, 1307–1317.

Bejsovec,A. and Anderson,P. (1990) Functions of the myosin ATP and actin binding sites are required for *C. elegans* thick filament assembly. *Cell*, **60**, 133–140.

Bernstein,S.I. and Milligan,R.A. (1997) Fine tuning a molecular motor: the location of alternative domains in the *Drosophila* myosin head. *J. Mol. Biol.*, **271**, 1–6.

Bernstein,S.I., Hansen,C.J., Becker,K.D., Wassenberg,D.R.,II, Roche,E.S., Donady,J.J. and Emerson,C.P.,Jr (1986) Alternative RNA splicing generates transcripts encoding a thorax-specific isoform of *Drosophila melanogaster* myosin heavy chain. *Mol. Cell. Biol.*, **6**, 2511–2519.

Burns,C.G., Larochelle,D.A., Erickson,H., Reedy,M. and De Lozanne,A. (1995) Single-headed myosin II acts as a dominant negative mutation in *Dictyostelium*. *Proc. Natl Acad. Sci. USA*, **92**, 8244–8248.

Butler-Browne,G.S. and Whalen,R.G. (1984) Myosin isozyme transitions occurring during the postnatal development of the rat soleus muscle. *Dev. Biol.*, **102**, 324–334.

Carpenter,J.M. (1950) A new semisynthetic food medium for *Drosophila*. *Drosoph. Inform. Serv.*, **24**, 96–97.

Collier,V.L., Kronert,W.A., O'Donnell,P.T., Edwards,K.A. and Bernstein,S.I. (1990) Alternative myosin hinge regions are utilized in a tissue-specific fashion that correlates with muscle contraction speed. *Genes Dev.*, **4**, 885–895.

Cripps,R.M. and Sparrow,J.C. (1992) Polymorphism in an indirect flight muscle-specific tropomyosin isozyme does not affect flight ability. *Biochem. Genet*., **30**, 156–165.

Cripps,R.M., Becker,K.D., Mardahl,M., Kronert,W.A., Hodges,D. and Bernstein,S.I. (1994) Transformation of *Drosophila melanogaster* with the wild-type myosin heavy chain gene: rescue of mutant phenotypes and analysis of defects caused by overexpression. *J. Cell Biol.*, **126**, 689–699.

Davis,J.S. (1988) Assembly processes in vertebrate skeletal thick filament formation. *Annu. Rev. Biophys. Chem.*, **17**, 217–239.

Drummond,D.R., Hennessey,E.S. and Sparrow,J.C. (1991) Characterisation of missense mutations in the *Act88F* gene of *Drosophila melanogaster*. *Mol. Gen. Genet.*, **226**, 70–80.

Epstein,H.F. and Fischman, D.A. (1991) Molecular analysis of protein assembly in muscle development. *Science*, **251**, 1039–1044.

Fernandes,J., Bate,M. and Vijayraghavan,K. (1991) Development of the indirect flight muscles of *Drosophila*. *Development*, **113**, 67–77.

Fyrberg,E., Karlik,C.C., Beall,C. and Saville,D.L. (1990) *Drosophila melanogaster* troponin-T mutations engender three distinct syndromes of myofibrillar abnormalities. *J. Mol. Biol.*, **216**, 657–675.

Fyrberg,C.C., Labeit,S., Bullard,B., Leonard,K. and Fyrberg,E. (1992) *Drosophila* projectin: relatedness to titin and twitchin and correlation with *lethal(4) 102 CDa* and *bent-Dominant* mutants. *Proc. R. Soc. London B*, **249**, 33–40.

George,E.L., Ober,M.B. and Emerson,C.P.,Jr (1989) Functional domains of the *Drosophila melanogaster* muscle myosin heavy-chain gene are encoded by alternatively spliced exons. *Mol. Cell. Biol.*, **9**, 2957–2974.

Geyer,P.K. and Fyrberg,E.A. (1986) 5′-flanking sequence required for regulated expression of a muscle-specific *Drosophila melanogaster* actin gene. *Mol. Cell. Biol.*, **6**, 3388–3396.

Hess,N.K. and Bernstein,S.I. (1991) Developmentally regulated alternative splicing of *Drosophila* myosin heavy chain transcripts: *in vivo* analysis of an usual 3′ splice site. *Dev. Biol.*, **146**, 339–344.

Hiromi,Y. and Hotta,Y. (1985) Actin gene mutations in *Drosophila*: heat shock activation in the indirect flight muscles. *EMBO J.*, **4**, 1681–1687.

Hodges,D., Cripps,R.M., O'Connor,M.E. and Bernstein,S.I. (1999) The role of evolutionarily conserved sequences in alternative splicing at the 3′ end of *Drosophila melanogaster* myosin heavy chain RNA. *Genetics*, **151**, 263–276.

Hoppe,P.E. and Waterston,R.H. (1996) Hydrophobicity variations along the surface of the coiled-coil rod may mediate striated muscle myosin assembly in *Caenorhabditis elegans*. *J. Cell Biol.*, **135**, 371–382.

Houmeida,A., Holt,J., Tskhovrebova,L. and Trinick,J. (1995) Studies of the interaction between titin and myosin. *J. Cell Biol.*, **131**, 1471–1481.

Huxley,H.E. (1963) Electron microscope studies on the structure of natural and synthetic proteins from striated muscle. *J. Mol. Biol.*, **7**, 281–308.

Kazzaz,J.A. and Rozek,C.E. (1989) Tissue-specific expression of the alternately processed *Drosophila* myosin heavy-chain messenger RNAs. *Dev. Biol.*, **133**, 550–561.

Kiehart,D.P. and Feghali,R. (1986) Cytoplasmic myosin from *Drosophila melanogaster*. *J. Cell Biol.*, **103**, 1517–1525.

Kronert,W.A., O'Donnell,P.T. and Bernstein,S.I. (1994) A charge change in an evolutionarily-conserved region of the myosin globular head prevents myosin and thick filament accumulation in *Drosophila*. *J. Mol. Biol.*, **236**, 697–702.

Kronert,W.A., O'Donnell,P.T., Fieck,A., Lawn,A., Vigoreaux,J.O., Sparrow,J.C. and Bernstein,S.I. (1995) Defects in the *Drosophila* myosin rod permit sarcomere assembly but cause flight muscle degeneration. *J. Mol. Biol.*, **249**, 111–125.

Labeit,S., Gautel,M., Lakey,A. and Trinick,J. (1992) Towards a molecular understanding of titin. *EMBO J.*, **11**, 1711–1716.

Laemmli,U.K. (1970) Cleavage of structural proteins during the assembly of the head of bacteriophage T4. *Nature*, **227**, 680–685.

Lindsley,D.L. and Zimm,G. (1992) *The Genome of Drosophila melanogaster.* Academic Press, San Diego, CA.

Lowey,S., Slayter,H.S., Weeds,A.G. and Baker,H. (1969) Substructure of the myosin molecule. I. Subfragments of myosin by enzymic degradation. *J. Mol. Biol.*, **42**, 1–29.

Machado,C., Sunkel,C.E. and Andrew,D.J. (1998) Human autoantibodies reveal titin as a chromosomal protein. *J. Cell Biol.*, **141**, 321–333.

Maeda,K., Sczakiel,G., Hofmann,W., Menetret,J.-F. and Wittinghofer,A. (1989) Expression of native rabbit light meromyosin in *Escherichia coli*. Observation of a powerful internal translation initiation site. *J. Mol. Biol.*, **205**, 269–273.

Moos,C., Offer,G., Starr,R. and Bennett,P. (1975) Interaction of C-protein with myosin, myosin rod and light meromyosin. *J. Mol. Biol.*, **97**, 1–9.

Nyitray,L., Mocz,G., Szilagyi,L., Balint,M., Lu,R.C., Wong,A. and Gergely,J. (1983) The proteolytic substructure of light meromyosin. *J. Biol. Chem.*, **258**, 13213–13220.

Obermann,W.M.J., Gautel,M., Weber,K. and Furst,D.O. (1997) Molecular structure of the sarcomeric M-band: mapping of titin and myosin binding domains in myomesin and the identification of a potential regulatory phosphorylation site in myomesin. *EMBO J.*, **16**, 211–220.

O'Donnell,P.T. and Bernstein,S.I. (1988) Molecular and ultrastructural defects in a *Drosophila* myosin heavy chain mutant: differential effects on muscle function produced by similar thick filament abnormalities. *J. Cell Biol.*, **107**, 2601–2612.

Peckham,M., Molloy,J.E., Sparrow,J.C. and White,D.C.S. (1990) Physiological properties of the dorsal longitudinal flight muscle and the tergal depressor of the trochanter muscle of *Drosophila melanogaster*. *J. Muscle Res. Cell Motil.*, **11**, 203–215.

Rayment,I., Rypniewski,W.R., Schmidt-Base,K., Smith,R., Tomchick,D.R., Benning,M.M., Winkelmann,D.A., Wesenberg,G. and Holden,H.M. (1993a) Three-dimensional structure of myosin subfragment-1: a molecular motor. *Science*, **261**, 50–58.

Rayment,I., Holden,H.M., Whittaker,M., Yohn,C.B., Lorenz,M., Holmes,K.C. and Milligan,R.A. (1993b) Structure of the actin–myosin complex and its implications for muscle contraction. *Science*, **261**, 58–65.

Reedy,M.C. and Beall,C. (1993) Ultrastructure of developing flight muscle in *Drosophila*. I. Assembly of myofibrils. *Dev. Biol.*, **160**, 443–465.

Reedy,M.C., Reedy,M.K., Leonard,K.R. and Bullard,B. (1994) Gold/Fab immuno electron microscopy localization of troponin H and troponin T in *Lethocerus* flight muscle. *J. Mol. Biol.*, **239**, 52–67.

Robertson,H.M., Preston,C.R., Phillis,R.W., Johnson-Schlitz,D.M., Benz,W.K. and Engels,W.R. (1988) A stable genomic source of *P* element transposase in *Drosophila melanogaster*. *Genetics*, **118**, 461–470.

Rozek,C.E. and Davidson,N. (1986) Differential processing of RNA transcribed from the single-copy *Drosophila* myosin heavy chain gene produces four mRNAs that encode two polypeptides. *Proc. Natl Acad. Sci. USA*, **83**, 2128–2132.

Rubin,G.M. and Spradling, A.C. (1982) Genetic transformation of *Drosophila* with transposable element vectors. *Science*, **218**, 348–353.

Sambrook,J., Fritsch,E.F. and Maniatis,T. (1989) *Molecular Cloning: A Laboratory Manual*. 2nd edn. Cold Spring Harbor Laboratory Press, Cold Spring Harbor, NY.

Seiler,S.H., Fischman,D.A. and Leinwand,L.A. (1996) Modulation of myosin filament organization by C-protein family members. *Mol. Biol. Cell*, **7**, 113–127.

Sohn,R.L., Vikstrom,K.L., Strauss,M., Cohen,C., Szent-Gyorgyi,A.G. and Leinwand,L.A. (1997) A 29 residue region of the sarcomeric myosin rod is necessary for filament formation. *J. Mol. Biol.*, **266**, 317–330.

Standiford,D.M., Davis,M.B., Miedema,K., Franzini-Armstrong,C. and Emerson,C.P.,Jr (1997) Myosin rod protein: a novel thick filament component of *Drosophila* muscle. *J. Mol. Biol.*, **265**, 40–55.

Vigoreaux,J.O., Hernandez,C., Moore,J., Ayer,G. and Maughan D. (1998) A genetic deficiency that spans the flightin gene of *Drosophila melanogaster* affects the ultrastructure and function of the flight muscles. *J. Exp. Biol.*, **201**, 2033–2044.

Vikstrom,K.L., Seiler,S.H., Sohn,R.L., Strauss,M., Weiss,A., Welikson,R.E. and Leinwand,L.A. (1997) The vertebrate myosin heavy chain: genetics and assembly properties. *Cell Struct. Funct.*, **22**, 123–129.

Wang,S.M., Jeng,C.J. and Sun,M.C. (1992) Studies on the interaction between titin and myosin. *Histol. Histopathol.*, **7**, 333–337.

Wells,L., Edwards,K.A. and Bernstein,S. I. (1996) Myosin heavy chain isoforms regulate muscle function but not myofibril assembly. *EMBO J.*, **15**, 4454–4459.

Whalen,R.G., Sell,S.M., Butler-Browne,G.S., Schwartz,K., Bouveret,P. and Pinset-Harstrom,I. (1981) Three myosin heavy-chain isozymes appear sequentially in rat muscle development. *Nature*, **292**, 805–809.

Wray,J.S. (1979) Filament geometry and the activation of insect flight muscles. *Nature*, **280**, 325–326.

Received October 8, 1998; revised and accepted February 12, 1999